



Universiteit
Leiden
The Netherlands

Rev1 deficiency induces replication stress to cause metabolic dysfunction differently in males and females

Panhuis, W.I.H.; Tsaalbi-Shtylik, A.; Schonke, M.; Harmelen, V. van; Pronk, A.C.M.; Streefland, T.C.M.; ... ; Kooijman, S.

Citation

Panhuis, W. I. H., Tsaalbi-Shtylik, A., Schonke, M., Harmelen, V. van, Pronk, A. C. M., Streefland, T. C. M., ... Kooijman, S. (2022). Rev1 deficiency induces replication stress to cause metabolic dysfunction differently in males and females. *Ajp - Endocrinology And Metabolism*, 322(3), E319-E329. doi:10.1152/ajpendo.00357.2021

Version: Not Applicable (or Unknown)

License: [Licensed under Article 25fa Copyright Act/Law \(Amendment Taverne\)](#)

Downloaded from: <https://hdl.handle.net/1887/3479794>

Note: To cite this publication please use the final published version (if applicable).

RESEARCH ARTICLE

Rev1 deficiency induces replication stress to cause metabolic dysfunction differently in males and females

 **Wietse In het Panhuis**,^{1,2} **Anastasia Tsaalbi-Shtylik**,³ **Milena Schönke**,^{1,2} **Vanessa van Harmelen**,^{2,3} **Amanda C. M. Pronk**,^{1,2} **Trea C. M. Streefland**,^{1,2} **Hetty C. M. Sips**,^{1,2} **Salwa Afkir**,^{1,2} **Ko Willems van Dijk**,^{1,2,3} **Patrick C. N. Rensen**,^{1,2} **Niels de Wind**,³ and  **Sander Kooijman**^{1,2}

¹Division of Endocrinology, Department of Medicine, Leiden University Medical Center, Leiden, The Netherlands; ²Eindhoven Laboratory for Experimental Vascular Medicine, Leiden University Medical Center, Leiden, The Netherlands; and ³Department of Human Genetics, Leiden University Medical Center, Leiden, The Netherlands

Abstract

DNA damage responses compete for cellular resources with metabolic pathways, but little is known about the metabolic consequences of impaired DNA replication, a process called replication stress. Here we characterized the metabolic consequences of DNA replication stress at endogenous DNA lesions by using mice with a disruption of Rev1, a translesion DNA polymerase specialized in the mutagenic replication of damaged DNA. Male and female Rev1 knockout (KO) mice were compared with wild-type (WT) mice and followed over time to study the natural course of body weight gain and glucose tolerance. Follow-up measurements were performed in female mice for in-depth metabolic characterization. Body weight and fat mass were only increased in female KO mice versus WT mice, whereas glucose intolerance and a reduction in lean mass were observed in both sexes. Female KO mice showed reduced locomotor activity while male KO mice showed increased activity as compared with their WT littermates. Further characterization of female mice revealed that lipid handling was unaffected by Rev1 deletion. An increased respiratory exchange ratio, combined with elevated plasma lactate levels and increased hepatic gluconeogenesis indicated problems with aerobic oxidation and increased reliance on anaerobic glycolysis. Supplementation with the NAD⁺ precursor nicotinamide riboside to stimulate aerobic respiration failed to restore the metabolic phenotype. In conclusion, replication stress at endogenous DNA lesions induces a complex metabolic phenotype, most likely initiated by muscular metabolic dysfunction and increased dependence on anaerobic glycolysis. Nicotinamide riboside supplementation after the onset of the metabolic impairment did not rescue this phenotype.

NEW & NOTEWORTHY An increasing number of DNA lesions interferes with cellular replication leading to metabolic inflexibility. We utilized Rev1 knockout mice as a model for replication stress, and show a sex-dependent metabolic phenotype, with a pronounced reduction of lean mass and glucose tolerance. These data indicate that in obesity, we may end up in an infinite loop where metabolic disturbance promotes the formation of DNA lesions, which in turn interferes with cellular replication causing further metabolic disturbances.

adiposity; anaerobic glycolysis; hyperglycemia; skeletal muscle

INTRODUCTION

Every cell acquires thousands of endogenous DNA lesions per day as the result of chemical reactions with reactive oxygen species and other reactive biomolecules and by spontaneous decay (1). Most of these endogenous DNA lesions are repaired by base excision repair and nucleotide excision repair. However, DNA lesions that have escaped repair interfere with genome duplication by arresting replicative DNA polymerases, which provokes replication stress. When replication stress threatens the integrity of the genome, DNA damage signaling induces DNA damage responses, including cell cycle arrests, cellular senescence, or apoptosis (2). Alternatively, the DNA lesion that induces replication stress

can be bypassed by a process referred to as translesion DNA synthesis (TLS) which allows for direct, but mutagenic, replication of DNA lesions (3). Rev1 is one of the TLS polymerases, catalyzing the direct incorporation of C nucleotides at abasic sites. In addition, Rev1 plays a structural role in TLS of severely helix-distorting exogenous and endogenous DNA lesions (3–5), by acting as a scaffold through interaction with other TLS polymerases and replication accessory factors (4, 6). TLS enables DNA damage tolerance, mitigating DNA damage signaling and thereby helps evading senescence and apoptosis and preserving the integrity of proliferating tissues (7), but by virtue of its inherent mutagenic nature, contributes to the etiology of several types of cancer (8).

Correspondence: W. In het Panhuis (w.in_het_panhuis@lumc.nl).

Submitted 8 October 2021 / Revised 25 January 2022 / Accepted 9 February 2022

<http://www.ajpendo.org>

0193-1849/22 Copyright © 2022 the American Physiological Society.



E319

A reciprocal interaction exists between ineffective DNA damage repair and aging-associated metabolic imbalances (1). An increased number of endogenous DNA lesions are present in individuals with obesity, possibly as a result of enhanced reactive oxygen species production and inflammation. These presumably induce chronic replication stress and consequent DNA damage responses that are associated with metabolic dysfunction (9–11). Interestingly, we previously demonstrated that Rev1 deficiency leads to increased oxidative stress and mitochondrial dysfunction as a result of rapid NAD⁺ depletion by poly(ADP) ribose polymerase 1 (PARP1) (7, 12), a key enzyme involved in detection and repair of damaged DNA and that this effect could be rescued by NAD⁺ precursor nicotinamide riboside (NR) supplementation (12, 13). Here we aimed to further elucidate the metabolic consequences of replication stress at endogenous DNA lesions by using Rev1 KO mice. We report that Rev1 KO mice have lower lean mass accompanied by glucose intolerance. Specifically in female mice, we observed a pronounced increase in fat mass. Mechanistically, we found evidence for a mitochondrial energy deficit associated with increased anaerobic glycolysis and reduced locomotor activity. NR supplementation after the onset of metabolic dysfunction did not rescue this phenotype.

MATERIALS AND METHODS

Animals

All experiments were conducted in accordance with the Institute for Laboratory Animal Research Guide for the Care and Use of Laboratory Animals and were approved by the National Committee for Animal experiments by the Ethics Committee on Animal Care and Experimentation of the Leiden University Medical Center. *Rev1*^{-/-} (referred to as Rev1 KO) mice on an FVB-C57BL/6J hybrid background were obtained as previously described (14) and compared with their wild-type (WT) littermates. All mice were housed under standard conditions at 21°C with a 12:12-h light-dark cycle and had ad libitum access to water and standard chow diet (Rat and Mouse No. 3 Breeding, SDS, Horley, UK) unless stated otherwise. Male mice were single-housed due to aggressive behavior of the Rev1 KO animals, whereas female mice were housed in groups of 2–4 mice/cage. In two sets of experiments, mice were followed over time and measurements were conducted at the indicated ages of the animals. In a third experiment, mice were either fed a standard chow diet or a diet enriched with NR (650 mg/kg body wt; Chromadex, Los Angeles, CA) for a total of 6 wk. Body weight and composition were monitored throughout all studies by a scale and EchoMRI (EchoMRI, Houston, TX), respectively. Mice were killed with CO₂, perfused transcardially with ice-cold phosphate-buffered saline for 5 min, and organs were collected for further analyses.

Plasma Assays

Mice were fasted for 4 h and plasma glucose was measured by Accu-Chek Aviva (Roche Diagnostics GmbH, Mannheim,

Germany) and plasma insulin by Ultra Sensitive Mouse Insulin ELISA Kit (90080, Crystal Chem, Downers Grove, IL).

Glucose Tolerance Tests

Mice were fasted for 4 h and baseline plasma glucose was measured before glucose was injected (2 g/kg lean mass). Plasma glucose levels were monitored over 2 h by Accu-Chek Aviva (Roche Diagnostics GmbH, Mannheim, Germany). In *experiment 3*, seven mice were excluded from the incremental area under the curve calculation as one timepoint was missing.

Lipid Tolerance Test

Mice were fasted for 4 h and baseline plasma was collected before animals received an olive oil bolus of 200 µL by oral gavage. Blood was sampled over 6 h for the measurement of plasma triglyceride (TG) concentrations.

Indirect Calorimetry

Mice were temporarily individually housed in automated metabolic home cages (Promethion System, Sable Systems, Berlin, Germany). O₂ consumption, CO₂ production, and voluntary locomotor behavior (by beam breaks) were continuously measured in 5 min bins and energy expenditure and respiratory exchange ratio (RER) were calculated. Mice were acclimatized for at least 24 h before starting baseline measurements at 21°C and a subsequent cold challenge at 4°C. Rectal temperature was measured before and at regular intervals during the cold challenge.

Hyperinsulinemic-Euglycemic Clamp

Mice were fasted for 4 h and anesthetized with a mix of acepromazine (6.25 mg/kg; Neurotranq, Alfasan, Woerden, The Netherlands), midazolam (6.25 mg/kg; Dormicum, Alfasan, Woerden, The Netherlands), and fentanyl (0.31 mg/kg; Hameln Pharma, Hameln, Germany). Mice received a continuous tail vein infusion of D-[3-³H]-glucose for 1 h (1.2 µCi/h; NET331C250UC, PerkinElmer, Waltham, MA) to determine basal rates of glucose turnover. Subsequently, mice received a bolus of insulin (150 mU/kg; NovoRapid, Novo Nordisk, Bagsværd, Denmark) followed by continuous infusion of insulin (210 mU/h/kg) and D-[3-³H]-glucose (1.2 µCi/h) for a total of 90 min. A variable infusion of D-glucose (12.5% solution in saline) was adjusted to achieve euglycemia by monitoring plasma glucose levels every 5–10 min with Accu-Chek Aviva (Roche Diagnostics GmbH, Mannheim, Germany). After achieving euglycemia at ~50 min, mice received a 2[1-¹⁴C]-deoxyglucose bolus (NEC495A250UC, PerkinElmer, Waltham, MA; 5µCi) to assess insulin-stimulated glucose uptake by organs. After 90 min, mice were euthanized by cervical dislocation and various organs were collected and dissolved overnight at 56°C in 0.5 mL SOLVABLE (PerkinElmer, Waltham, MA). Subsequently, organs were diluted in 5 mL of Ultima Gold (PerkinElmer, Waltham, MA) and glucose uptake by organs was assessed by measuring ¹⁴C-activity with a β counter (PerkinElmer, Tri-Carb 2910 TR, Waltham, MA). Blood samples were collected through tail bleeding at *t* = 50 and 60 min during the basal period and at *t* = 70, 80, and 90 min during the

hyperinsulinemic period to determine plasma activity of D-[3-³H]glucose. Whole body glucose uptake and hepatic glucose production during the basal and hyperinsulinemic period, as well as the insulin sensitivity index, were calculated as previously described (15). Glucose uptake by organs was calculated as micromole per gram tissue. Two mice were excluded due to technical problems.

Triglyceride-Derived Fatty Acid Clearance and Uptake by Organs

Triglyceride (TG)-rich lipoprotein-like particles (80 nm) radiolabeled with glycerol tri[³H]oleate were prepared and characterized as described previously (16). Mice were fasted for 4 h and plasma was collected before an intravenous injection of lipoprotein-like particles (1 mg TG diluted in 200 μ L saline/mouse). Plasma was collected over time to determine plasma decay. After 15 min, mice were euthanized by CO₂ inhalation, perfused via the heart with ice-cold PBS, and various organs were collected. Organs were processed as described in *Hyperinsulinemic-Euglycemic Clamp* above and ³H-activity was measured with a β counter (Tri-Carb 2910 TR, PerkinElmer, Waltham, MA). The uptake by organs was calculated as a percentage of injected dose per whole organ.

Glycogen Content

Glycogen content of tibialis anterior was measured using the Glycogen Assay Kit II (Abcam, Cambridge, UK), according to the manufacturer's protocol.

Plasma Lactate and Alanine

Plasma lactate (kit ab65331) and alanine (kit ab83394) were measured after deproteinization with 10-kDa spin columns (kit ab93349) (all Abcam, Cambridge, UK), according to the manufacturer's protocols.

NAD⁺ Content in Skeletal Muscle

NAD⁺ content was measured in tibialis anterior muscle from WT and Rev1 KO mice supplemented with NR by using the NAD/NADH Quantification Kit (Sigma Aldrich, St. Louis, Missouri), after deproteinization with 10-kDa spin columns (ab93349), according to the manufacturer's protocols.

Gene Expression

Frozen interscapular brown adipose tissue (iBAT) was lysed in TriPure Isolation Reagent (Roche, Diagnostics, Almere, The Netherlands) for RNA isolation. Subsequently, cDNA was synthesized from 1 μ g RNA using M-MLV Reverse Transcriptase (Promega, Madison, WI) and qPCR was carried out using SYBR green kit (Promega, Madison, WI) on a CFX96 PCR machine (Bio-Rad, Hercules, CA), according to the manufacturer's protocols. mRNA expression was normalized to 60S acidic ribosomal protein P0 (*Rplp0*) as housekeeping gene and expressed as a fold change compared with the WT group using the $\Delta\Delta$ CT method. Primers are listed in Supplemental Table S1; see <https://doi.org/10.6084/m9.figshare.16774813>.

Mitochondrial-to-Nuclear DNA Ratio

Mitochondrial and nuclear DNA were isolated from tibialis anterior using the QIAamp DNA Mini Kit (No. 51306;

Qiagen, Hilden, Germany), according to the manufacturer's protocol. qPCR was carried out with 1 ng DNA using SYBR green kit (Promega, Madison, WI) on a CFX96 PCR machine (Bio-Rad, Hercules, CA), according to the manufacturer's protocols. Combined mRNA expression of mitochondrial genes 16S ribosomal RNA (*16S*) and cyclooxygenase 2 (*Cox2*) was normalized to nuclear genes hexokinase 2 (*Hk2*) and uncoupling protein 2 (*Ucp2*) and expressed as a fold change compared with the WT group using the $\Delta\Delta$ CT method. Primers are listed in Supplemental Table S2.

Protein Quantification

Frozen tissue was lysed in PI3K buffer and homogenized as described previously (17). Protein concentrations were determined using the Pierce bicinchoninic acid (BCA) Protein Assay Kit (Thermo Fisher Scientific, Waltham). Protein samples from fasted mice were used to measure mitochondrial oxidative phosphorylation complexes I-V by using Total OXPHOS Rodent WB Antibody Cocktail (ab110413; Abcam, Cambridge, UK; diluted 1:1,000) as described previously (17). Blots were stained with Ponceau S (5% Ponceau S in water with 2.5% acetic acid) for normalization. Protein samples from clamped mice were used to measure phosphorylated protein kinase B (pAKT)^{Thr308}, AKT (D6G4), phosphorylated-acetyl-CoA carboxylase (p-ACC)^{Ser79}, and ACC, and samples from fasted mice were used to measure citrate synthase by using automated Western blot with Wes (ProteinSimple, Santa Clara, CA), according to the manufacturer's protocol. Protein lysates were diluted to 0.8 μ g/ μ L for p-AKT and AKT, to 0.2 μ g/ μ L for p-ACC, ACC, and GAPDH, and to 0.02 μ g/ μ L for citrate synthase. For detection, phospho-Akt (Thr308; 1:20), Akt2 (D6G4) rabbit mAb (1:20), phospho-acetyl-CoA carboxylase (Ser79) antibody (1:20), acetyl-CoA carboxylase antibody (1:20) (9275, 3063, 3661, and 3662, respectively, Cell Signaling, Danvers, MA), and anti-citrate synthetase antibody (ab96600, Abcam, Cambridge, UK; 1:20) were used. GAPDH (1:50; sc-25778, Santa Cruz, Dallas, TX) was used for normalization. For all antibodies, a secondary anti-rabbit antibody (1:1,000, 10 μ L/well) was used. Compass software (ProteinSimple; v5.0.1) was used for analysis and quantification. An overview of all blot images is displayed in Supplemental Fig. S5.

Statistical Analyses

Statistical analyses between groups were performed with unpaired *t* tests, one-way or two-way ANOVA with post hoc tests, where applicable. Data sets were tested for normality. In case of non-normal distributions, nonparametric tests were performed (Mann-Whitney). Differences in energy expenditure between groups were analyzed by analysis of covariance (ANCOVA), listing lean mass, and locomotor activity as separate covariables. Data are presented as means (\pm SE). Differences at *P* < 0.05 were considered statistically significant. Statistical analyses were performed with GraphPad Prism software, version 8.4.2 (GraphPad, La Jolla, California) or SPSS Statistics 25 (IBM, Armonk, NY).

RESULTS

Rev1 Deficiency Induces Adiposity in Female Mice and Reduces Lean Mass Accompanied by Impaired Glucose Tolerance in Both Male and Female Mice

To study the impact of replication stress at endogenous DNA damage on the natural course of body weight gain, male and female Rev1 KO mice with an average age of 8 (4.5–11.5) wk of age were compared with their WT littermates and followed over time. Female Rev1 KO mice showed increased body weight gain (Fig. 1D; time-genotype interaction by two-way ANOVA: $P = 0.0001$) explained by an increase in fat mass over time (Fig. 1E; time-genotype interaction by two-way ANOVA: $P = 0.0001$). These parameters were unchanged in male Rev1 KO compared with WT mice (Fig. 1, A and B). However, both male and female Rev1 KO mice had significantly reduced lean mass when compared with their WT littermates throughout the course of the study (Fig. 1, C and F). There was a trend for reduced locomotor activity in female Rev1 KO mice (Fig. 1G; $P = 0.055$; measured in $n = 4$ mice), and a significant increase in male Rev1 KO mice, compared with their WT littermates (Supplemental Fig. S1A). At 25 (21.5–28.5) wk of age, female Rev1 KO mice had elevated glucose (Fig. 1H) and insulin levels (Fig. 1I) and they showed impaired glucose tolerance (Fig. 1, J and L). In males, Rev1 deficiency elevated fasting glucose levels but insulin levels were unchanged (Supplemental Fig. S1, B and C). Glucose clearance was slower in the male Rev1 KO mice suggesting impaired second phase insulin release (Supplemental Fig. S1, D–F), albeit less pronounced than in females. At an average age of 30 (26.5–33.5) wk, the mice were killed and organs were collected. Subcutaneous white adipose tissue (sWAT) weight was increased in female Rev1 KO mice (Fig. 1M) but not in the males (Supplemental Fig. S1G), in line with the differences in fat mass among the genotypes and sexes. Gonadal white adipose tissue (gWAT) and liver weight (Fig. 1M, Supplemental Fig. S1G) were unchanged by Rev1 deficiency in both sexes.

Rev1 Deficiency Does Not Affect Lipid Tolerance in Female Mice

As the female Rev1 KO mice showed a more pronounced metabolic phenotype than their male counterparts, we followed up on this sex to more comprehensively assess alterations in energy metabolism and delineate underlying mechanisms. In this second experiment, we plotted body weight and body composition by age to estimate the age of onset of the metabolic phenotype. Fat mass gain in female Rev1 KO mice was significantly increased from 11 wk of age onward, whereas lean mass was already reduced at the first measurement at 5 wk of age (Supplemental Fig. S2, A–C). Cumulative food intake, which was measured in $n = 3$ cages of 3 mice/genotype, was lower in Rev1 KO mice when compared with their WT littermates (Fig. 2A) regardless of correction for body weight (Supplemental Fig. S2D) or lean mass (Supplemental Fig. S2E), suggesting reduced energy demand. To investigate whether impaired lipid handling caused the increase in fat mass, we subjected half of the mice at 14 (11.5–16.5) wk of age to a lipid tolerance test (Fig. 2, B–D). Although the postprandial TG curves appeared

different between WT and Rev1 KO mice, there was no significant difference at any of the time points, nor for fasted TG levels. At 18 (15.5–20.5) wk of age, we injected the same subset of mice with TG-rich lipoprotein-like particles labeled with glycerol tri[^3H]oleate to assess plasma clearance and organ distribution of TG-derived fatty acids. In line with the unchanged lipid tolerance, plasma clearance of ^3H -activity did not differ between genotypes (Fig. 2E) and we could only detect a modest increase in [^3H]oleate uptake by the heart, but not by any of the other metabolic organs, in the Rev1 KO mice (Fig. 2F).

Rev1 Deficiency Decreases Energy Expenditure as a Consequence of Reduced Lean Mass and Locomotor Activity in Female Mice

To assess the consequences of Rev1 deficiency on whole body energy expenditure, the second half of the female mice was temporarily housed in metabolic cages at 17 (14.5–19.5) wk of age. The decreased food intake in Rev1 KO mice during this week (Supplemental Fig. S3A) was consistent with the reduced food intake we observed throughout the study (Fig. 2A). The Rev1 KO mice showed decreased energy expenditure (Fig. 2, G and H). This effect was most pronounced around the onset and during the first half of the dark phase and accompanied by a strong decrease in locomotor activity during this period (Fig. 2, K and L). Covariate analysis suggested that both the lower lean mass and the reduced locomotor activity contributed to the overall decrease in energy expenditure in the Rev1 KO mice (Supplemental Table S3). Interestingly, throughout the dark phase, the RER was substantially elevated in the Rev1 KO mice when compared with their WT littermates (Fig. 2, I and J), possibly due to an increase in anaerobic glycolysis in line with the previously reported mitochondrial dysfunction upon Rev1 deletion (12). During a cold challenge, the Rev1 KO mice were able to defend their core body temperature (Supplemental Fig. S3B) by increasing their energy expenditure (Supplemental Fig. S3, C and D) but relied more on fat oxidation as suggested by the low RER (Supplemental Fig. S3, E and F). Impaired carbohydrate oxidation, reduced lean mass, and reduced locomotor activity collectively suggest that the metabolic phenotype originates from skeletal muscle. To exclude the involvement of thermoregulatory BAT, we assessed functional markers in BAT. Consistent with the unchanged lipid tolerance and [^3H]oleate uptake by BAT and cold tolerance, the expression of genes involved in thermogenesis, mitochondrial function, glucose uptake, and lipid uptake in BAT was unchanged between the genotypes (Supplemental Fig. S3G).

Rev1 Deficiency Increases Hepatic Glucose Production and Insulin-Stimulated Glucose Uptake in Muscle in Female Mice

In the female mice subjected to indirect calorimetry, we performed a hyperinsulinemic-euglycemic clamp to delineate mechanisms underlying the glucose intolerance at 18 (15.5–20.5) wk of age. During both the basal (fasted) and hyperinsulinemic state, plasma glucose levels were higher in Rev1 KO mice compared with WT mice (Fig. 3A), whereas glucose infusion rates were comparable between genotypes

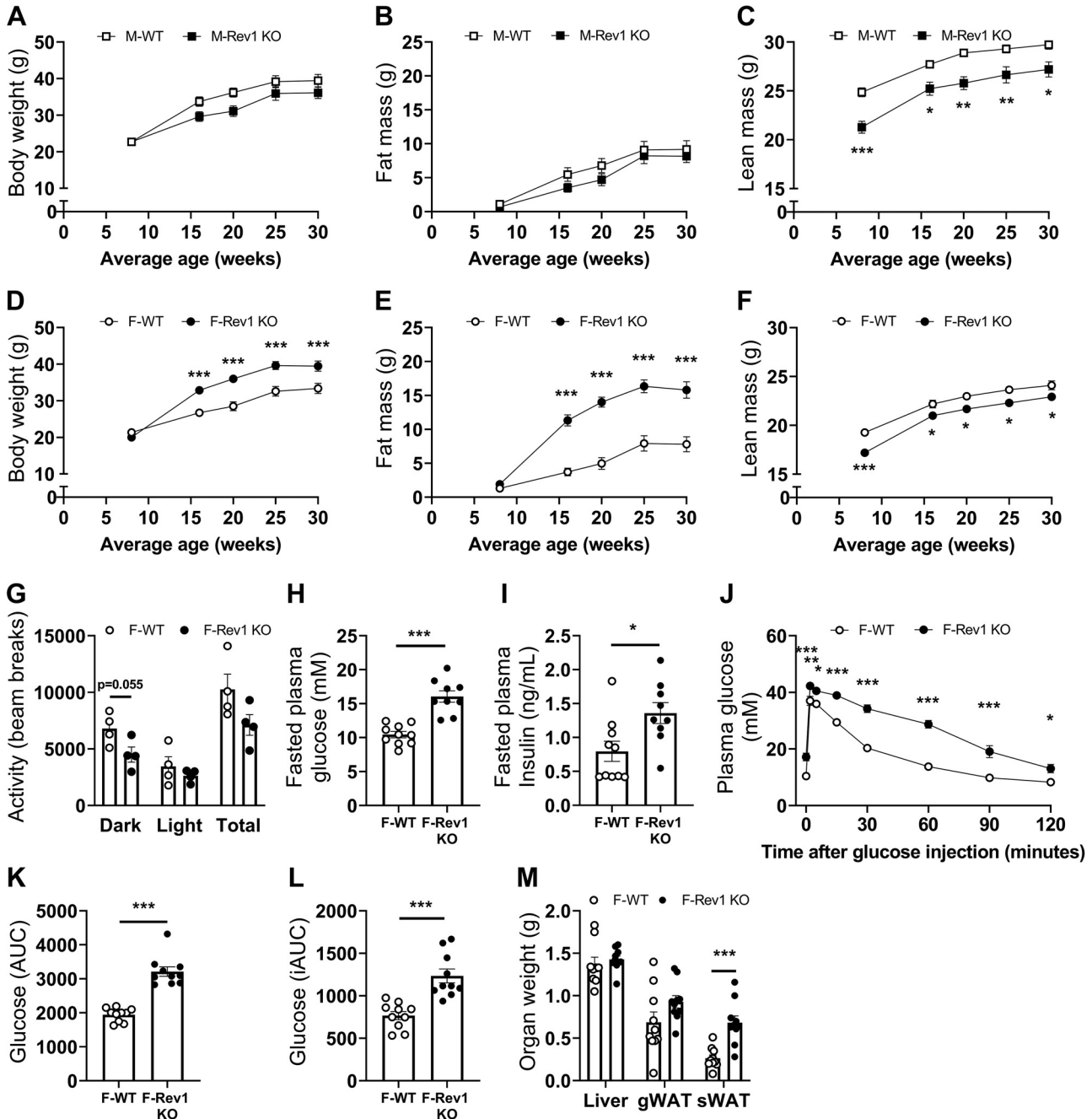


Figure 1. Body composition and glucose tolerance. Male WT (white square) and Rev1-KO (black square), and female WT (white circle or bar) and Rev1-KO (black circle or bar) were monitored during 22 wk starting at 8 (4.5–11.5) wk of age for (A/D) body weight, (B/E) fat mass, and (C/F) lean mass for males and females, respectively ($n = 8-10$ mice/group). G: voluntary locomotion behavior was recorded in female mice by measuring beam breaks with infrared passive cameras and expressed during the dark phase, light phase, and total in single-housed mice for 24 h ($n = 4$ mice). Female mice 25 (21.5–28.5) wk of age were fasted for 4 h, and (H) plasma glucose and (I) plasma insulin levels were measured, before injection with an intravenous glucose bolus at ZT6. J: plasma glucose was measured at $t = 2, 5, 10, 15, 30, 60, 90,$ and 120 min and (K) the area under the curve (AUC) and (L) the incremental AUC (iAUC) were calculated. M: liver, gonadal white adipose tissue (gWAT), and subcutaneous white adipose tissue (sWAT) of 30 (26.5–33.5)-wk-old female mice were weighed. Data are presented as means \pm SE ($n = 8-10$ mice/group). *WT vs. Rev1-KO. * $P < 0.05$; ** $P < 0.01$; *** $P < 0.001$, according to unpaired t test, two-way ANOVA and Šídák's multiple-comparisons test, or Mann-Whitney test. KO, knockout; WT, wild-type.

(Fig. 3B). Whole body [$3-^3\text{H}$]glucose utilization (Fig. 3C) and hepatic glucose production (Fig. 3D) were both significantly elevated during the basal state. Although hepatic glucose production remained nonsignificantly elevated in the hyperinsulinemic state, the relative suppression was comparable in both genotypes (Fig. 3E). The elevated

glucose levels during the glucose tolerance test (Fig. 1J) were thus explained by elevated hepatic glucose production rather than impaired glucose clearance. The whole body insulin sensitivity index, calculated based on the difference between the basal and hyper state, showed no significant changes in whole body or hepatic insulin

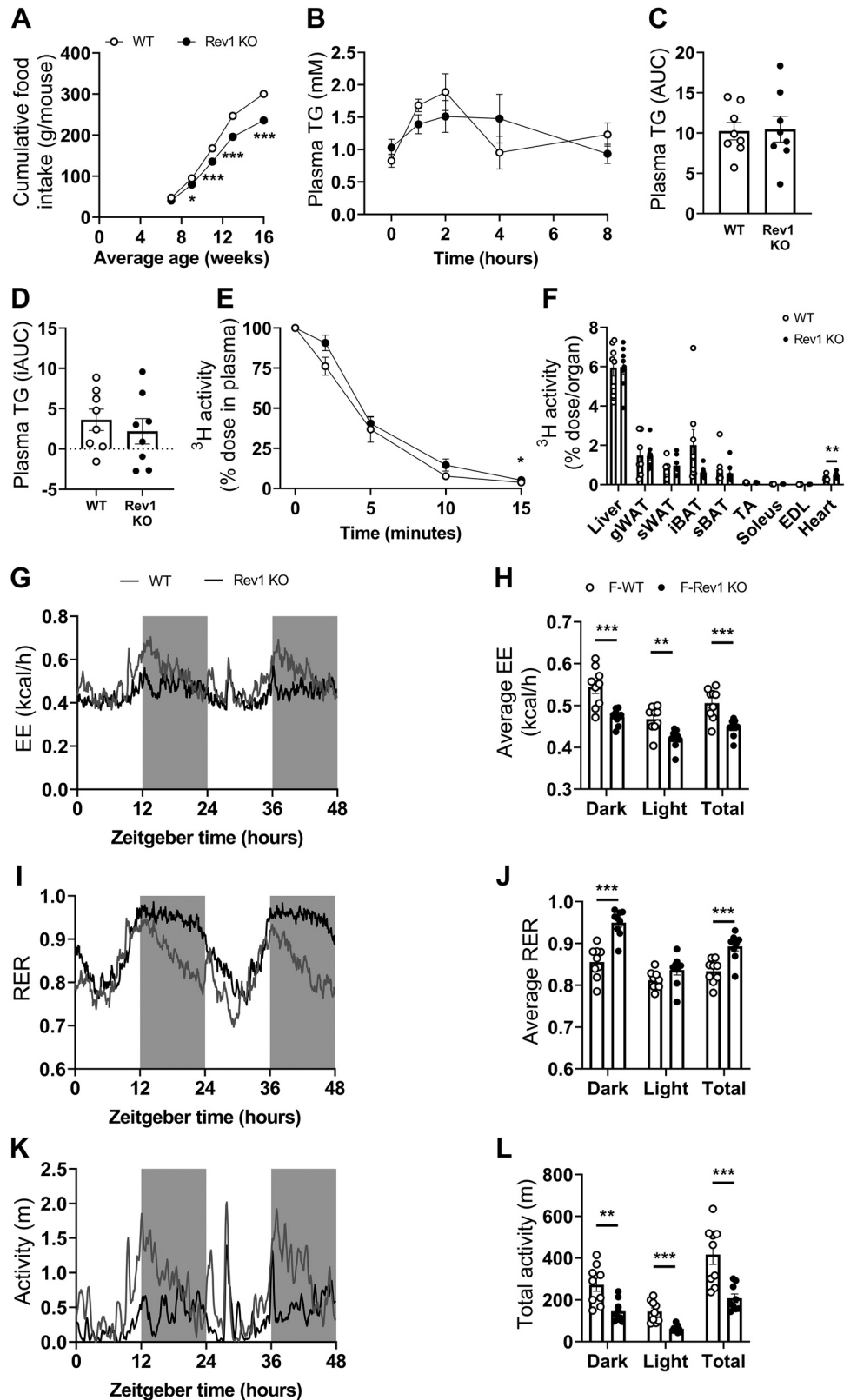
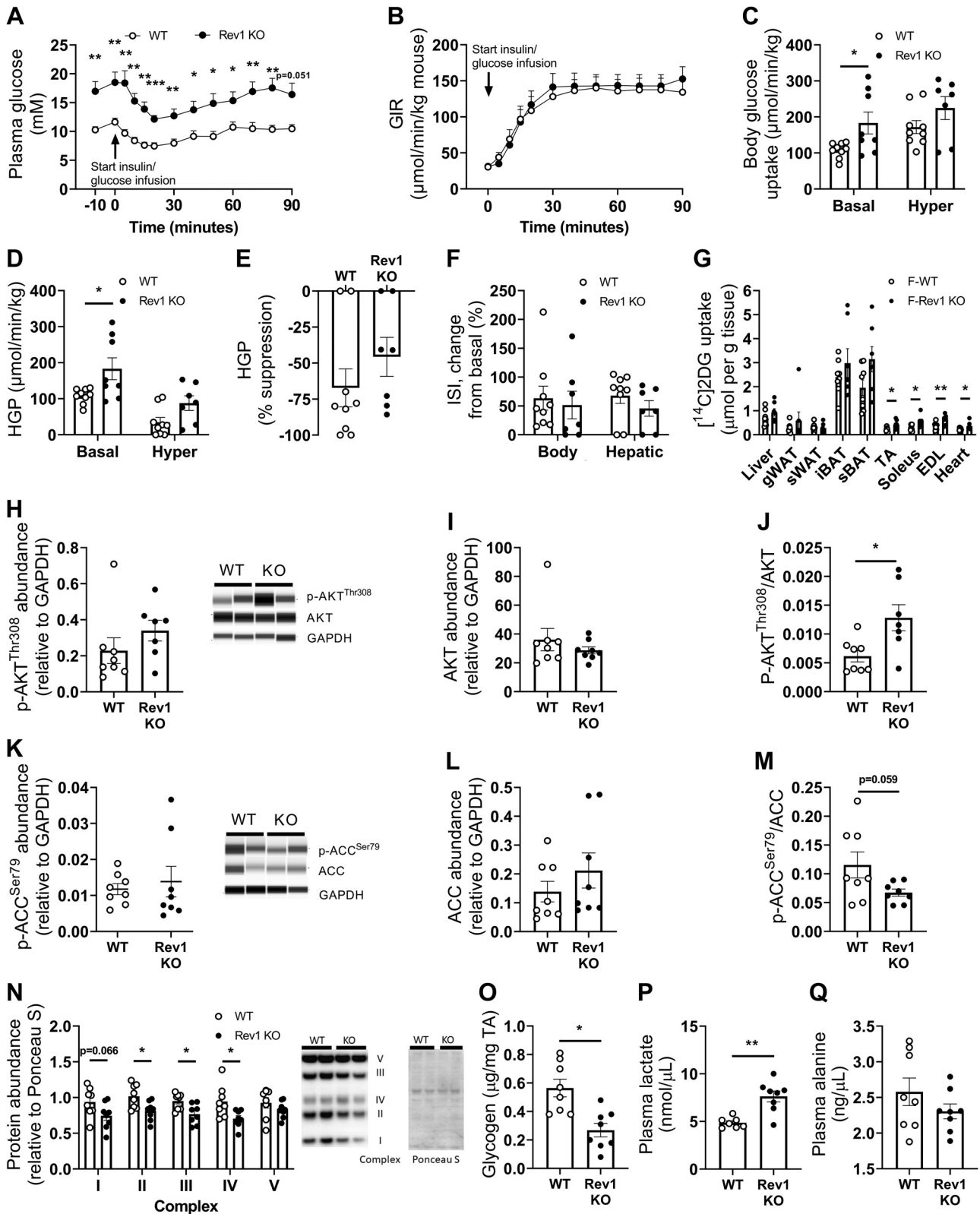


Figure 2. Lipid tolerance and indirect calorimetry. In female WT (white symbols) and Rev1-KO (black symbols) mice, (A) food intake was measured for 9 wk, starting at the age of 7 (4.5–9.5) wk ($n = 3$ cages of 3 mice). B: mice of 14 (11.5–16.5) wk old were fasted for 4 h and received an oral olive oil bolus at ZT12 and blood was collected for plasma TG measurement at $t = 0, 1, 2, 4,$ and 8 h ($n = 8$ mice/group), after which (C) the area under the curve (AUC) and (D) incremental AUC (iAUC) were calculated. Mice 18 (15.5–20.5) wk of age were fasted for 4 h and injected with very-low-density-lipoprotein-like TG-rich particles labeled with glycerol tri[³H]oleate at ZT12 to assess (E) plasma clearance and (F) uptake by gonadal white adipose tissue (gWAT), subcutaneous (sWAT), interscapular brown adipose tissue (iBAT), subscapular brown adipose tissue (sBAT), tibialis anterior (TA), soleus, extensor digitorum longus (EDL), and heart ($n = 8$ mice/group). Mice 17 (14.5–19.5) wk of age were single-housed in metabolic cages for continuous measurements of O₂ consumption and CO₂ production, from which (G and H) whole body energy expenditure (EE) and (I and J) respiratory exchange ratio (RER) were calculated during the dark phase, light phase, and combined. K and L: locomotor activity was assessed by beam breaks ($n = 9$ mice/group). Data are presented as means \pm SE. *WT vs. Rev1-KO. * $P < 0.05$; ** $P < 0.01$; *** $P < 0.001$, according to two-way ANOVA and Šídák's multiple-comparisons test. KO, knockout; TG, triglyceride; WT, wild-type.

sensitivity (Fig. 3F). However, insulin-stimulated glucose uptake as assessed by [¹⁴C]2DG uptake in clamped mice was elevated in all muscles (tibialis anterior, soleus, extensor digitorum longus, and heart) of Rev1 KO mice (Fig.

3G). Accordingly, insulin-stimulated p-AKT/AKT ratio was found to be increased in the tibialis anterior of Rev1 KO mice (Fig. 3, H–J). In line with this, p-ACC^{Ser79}/ACC ratio was nonsignificantly reduced ($P = 0.059$) (Fig. 3, K–



M), suggesting reduced β -oxidation as a consequence of elevated glucose availability.

Rev1 Deficiency Aggravates Oxidative Phosphorylation in Muscle While Inducing Anaerobic Glycolysis in Female Mice

As we previously showed that Rev1 deletion can cause mitochondrial dysfunction (7, 12) and the data obtained thus far point toward impaired skeletal muscle physiology, we measured protein abundance of the mitochondrial oxidative phosphorylation complexes I-V in the tibialis anterior from mice that were killed during the fasted state. Rev1 KO mice showed a significantly reduced abundance of complexes II, III, and IV, whereas the abundance of the complex I and V was nonsignificantly reduced (Fig. 3N). However, we were unable to detect any changes in other measures of mitochondrial quantity or quality, including mitochondrial/nuclear DNA ratio and citrate synthase abundance (Supplemental Fig. S3, H and I). Nevertheless, we did observe reduced glycogen content in the tibialis anterior (Fig. 3O) and significantly elevated plasma levels of lactate in the Rev1 KO mice (Fig. 3P), consistent with increased dependence on anaerobic glycolysis. Within the Cori cycle lactate is a substrate for hepatic gluconeogenesis and can thus promote hepatic glucose production that was indeed found to be increased (Fig. 3D). Plasma alanine, which can also serve as a substrate for gluconeogenesis, was unaltered (Fig. 3Q).

Dietary NR Supplementation Does Not Rescue the Metabolic Phenotype of Female Rev1 KO Mice

To test the hypothesis that NAD^+ repletion could inhibit or reverse the metabolic phenotype induced by Rev1 deficiency, 14 (12–16)-wk-old Rev1 KO mice and WT littermates received dietary NR for a total of 6 wk. NR supplementation nonsignificantly increased NAD^+ content in tibialis anterior (Fig. 4A) of WT ($P = 0.101$) and Rev1 KO mice ($P = 0.091$), and significantly increased NAD^+ content in liver of WT mice (Supplemental Fig. S4A). However, NR supplementation did not prevent body weight gain (Fig. 4B) or fat mass gain (Fig. 4C), nor did it prevent glucose intolerance at ZT5 at 18 (16–20) wk of age (Fig. 4, E and F).

DISCUSSION

In this study, we investigated the metabolic consequences of replication stress induced by deletion of Rev1. We showed that Rev1 deletion from a young age onward induces adiposity in females but not in male mice, although both sexes

showed reductions in lean mass accompanied by impaired glucose tolerance. Mechanistically, we found evidence for increased dependence on anaerobic glycolysis and excessive hepatic glucose production as such.

The complex metabolic phenotype of the Rev1 KO mice appears to be originating from impaired muscular metabolic function and increased reliance on anaerobic respiration (see also the graphical summary in Fig. 5). Mitochondrial NAD^+ depletion in Rev1 deficiency, as demonstrated previously (12), might have been responsible for these effects, although we only found limited direct evidence for mitochondrial dysfunction in skeletal muscle. Nonetheless, a cellular energy deficit due to reduced ability to complete the Krebs cycle or β -oxidation would explain the decreased glycogen content and increased insulin responsiveness of the muscle. In addition, increased reliance on anaerobic glycolysis may also account for the elevated circulating levels of lactate and increased hepatic glucose production, possibly explaining the elevated postprandial glucose excursions in the Rev1 KO mice. Furthermore, a possible decrease in skeletal muscle oxidative capacity can lead to breakdown of the tissue, aligning with the observed reduced lean mass, locomotor activity, and whole body energy expenditure.

In female, but not male Rev1 KO mice, fat mass was increased. We suspect that this difference between the sexes was due to higher locomotor activity in males consequential to an elevated stress response during handling of the male Rev1 KO mice and more aggressive behavior toward each other when compared with their WT littermates, hence the reason for single-housing of all male mice during our experiments. For future studies, it would be of interest to obtain more insight into the sexual dimorphic behavioral changes caused by Rev1 deficiency and how these relate to the metabolic phenotype.

Replication stress theoretically occurs in all proliferating cells, yet we found no evidence for primary functional impairment in metabolic organs other than skeletal muscle, such as BAT and WAT. Lipid tolerance and distribution were unaffected, as was insulin-stimulated glucose uptake by the adipose tissues. This could explain why Rev1 deletion increases RER at room temperature and reduces RER during cold exposure compared with their WT littermates. A higher RER at room temperature is likely a consequence of increased reliance on anaerobic glycolysis in muscle, whereas the relative contribution of fat oxidation by BAT to total energy expenditure during cold likely further increases because Rev1 KO mice cannot rely on (non)shivering thermogenesis in muscle. Interestingly, deficiency of another

Figure 3. Insulin sensitivity and mitochondrial complex abundance. Female WT (white symbols) and Rev1-KO mice (black symbols), 18 (15.5–20.5) wk of age, were fasted for 4 h and subjected to a hyperinsulinemic-euglycemic clamp at ZT7. During both the basal and hyperinsulinemic period, (A) plasma glucose was monitored every 5–10 min, and (B) the glucose infusion rate (GIR) was adjusted accordingly. A [$3\text{-}^3\text{H}$]glucose label was used to measure (C) the whole body glucose uptake and (D) hepatic glucose production (HGP) during the basal and hyperinsulinemic period. The difference between both periods was used to calculate (E) the relative hepatic glucose suppression (F) and the whole body and hepatic insulin sensitivity index (SI) ($n = 7\text{--}9$ mice/group). [^{14}C]2deoxyglucose was injected at 50 min after the start of the insulin infusion and (G) organ distribution was assessed in liver, gonadal white adipose tissue (gWAT), subcutaneous (s)WAT, interscapular brown adipose tissue (iBAT), subscapular (s)BAT, tibialis anterior (TA), soleus, extensor digitorum longus (EDL), and heart ($n = 7$ or 8 mice/group). Protein abundance of (H) p-AKT^{Thr308}, (I) AKT, (K) p-ACC^{Ser79}, and (L) ACC in TA of clamped mice were analyzed by automated Western blot with Wes to calculate (J) p-AKT^{Thr308}/AKT and (M) p-ACC^{Ser79}/ACC ratio. N: protein abundance of mitochondrial oxidative phosphorylation (OXPHOS) complexes I-V in tibialis anterior (TA) from fasted female WT and Rev1 KO mice 20 (18–22) wk of age was analyzed by Western blot on two gels that were derived and processed at the same time and normalized to a loading marker. O: glycogen content in TA, (P) plasma lactate, and (Q) plasma alanine were measured in the same mice ($n = 7$ or 8 mice/group). Data are presented as means \pm SE. *WT vs. Rev1-KO. * $P < 0.05$; ** $P < 0.01$; *** $P < 0.001$, according to unpaired t test or two-way ANOVA and Sidák's multiple-comparisons test. KO, knockout; WT, wild-type.

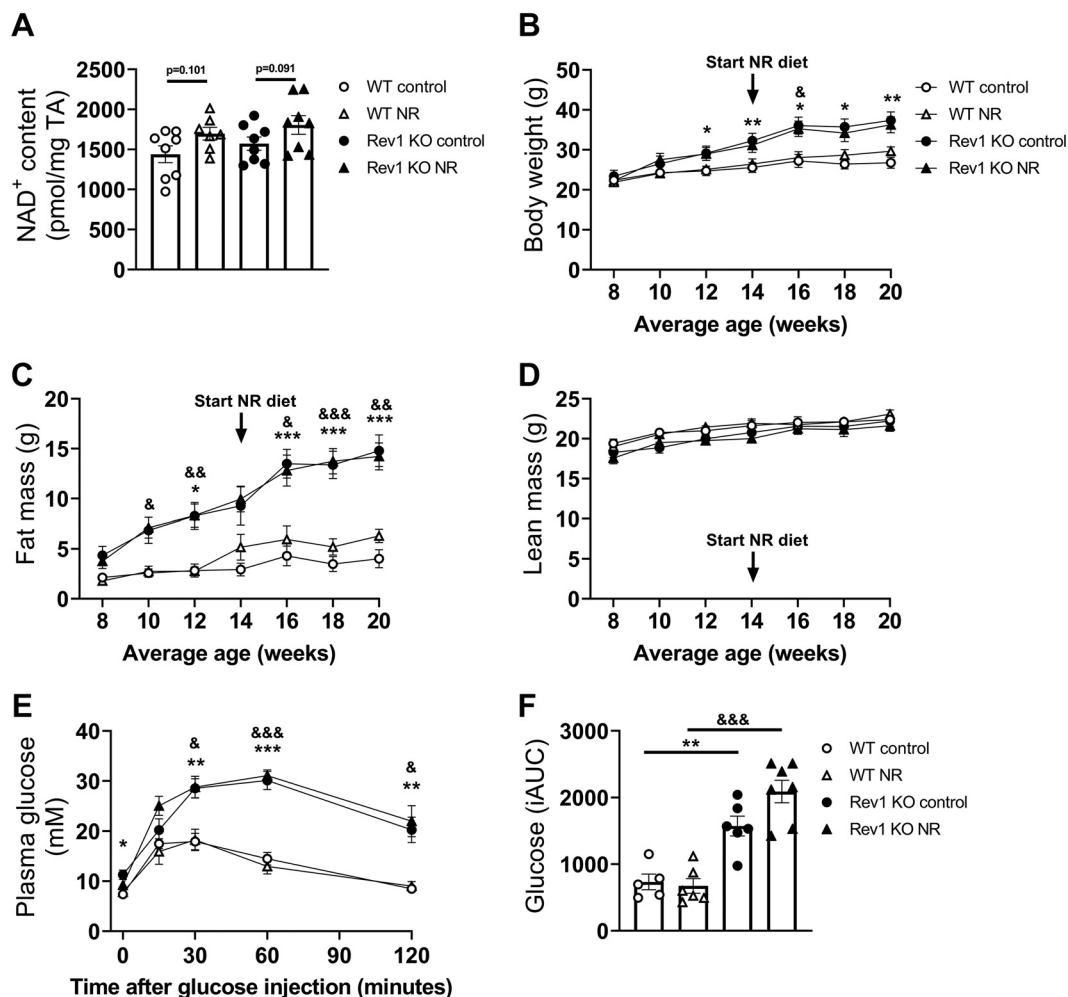


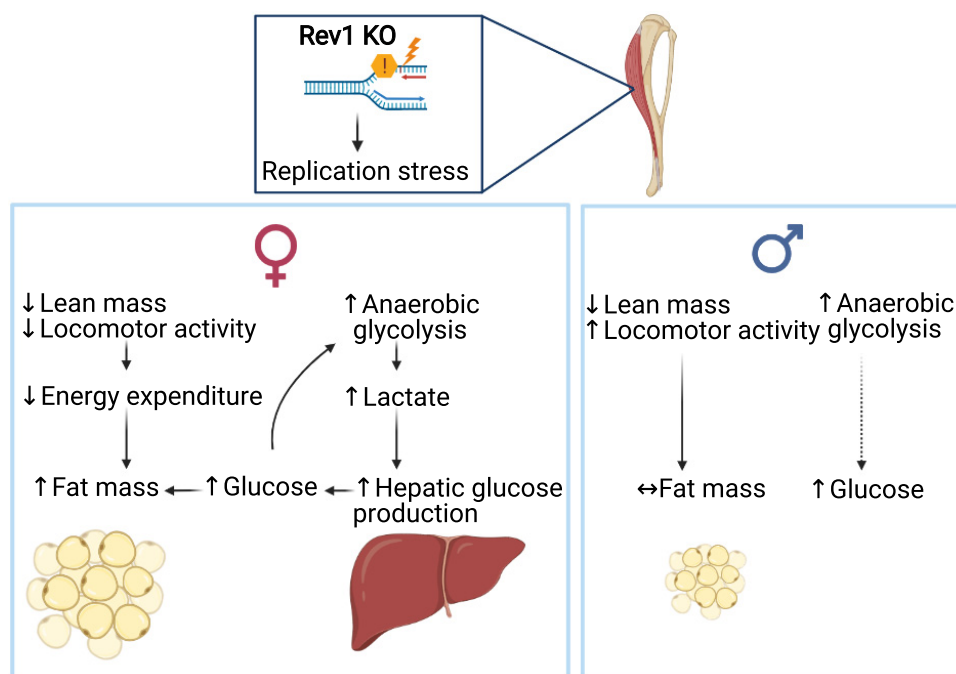
Figure 4. Nicotinamide riboside supplementation. Female WT (white symbols) and Rev1 KO mice (black symbols) received dietary nicotinamide riboside for 6 wk starting at the age of 14 (12–16) wk. **A:** NAD⁺ content in tibialis anterior (TA) was analyzed and **(B)** body weight, **(C)** fat mass, and **(D)** lean mass were monitored throughout the study. Mice 18 (16–20) wk of age were fasted for 4 h and injected with an intraperitoneal glucose bolus at ZT5. **E:** plasma glucose was measured prior to injection and at $t = 15, 30, 60,$ and 120 min and **(F)** the incremental area under the curve (iAUC) was calculated. Data presented as means \pm SE ($n = 7$ or 8 mice/group). Circles indicate control groups, triangles indicate NR-treated groups. *WT control vs. Rev1-KO control. &WT NR vs. Rev1 KO NR. *, &P < 0.05; **, &P < 0.01; ***, &P < 0.001, according to two-way ANOVA and Šidák's multiple-comparisons test. KO, knock-out; NR, nicotinamide riboside; WT, wild-type.

TLS polymerase, polymerase η , was recently reported to induce obesity and glucose intolerance that coincided with accelerated adipose tissue senescence (18). The development of obesity occurred later in life in polymerase η KO mice, whereas we observed increased adiposity in Rev1 KO mice from a young age onward. This difference between the models could possibly be explained by the different functions of the polymerases. Polymerase η is thought to be involved in bypassing poorly distorting lesions and Rev1 in bypassing severely distorting lesions. As impaired bypassing of severely distorting lesions results in more replication stress than poorly distorting lesions, Rev1 deficiency may cause greater replication stress than polymerase η deficiency, explaining why Rev1 deficiency induces a metabolic phenotype in early life and polymerase η deficiency does not. In line with this notion, previous studies using mouse models with genetic alterations in DNA repair and DNA damage response genes identified different tissues as the origin of metabolic dysfunction, such as impaired glucose homeostasis (9). For

example, Ataxia telangiectasia mutated (*Atm*)^{-/-} (19) and p44 (a short isoform of p53) (20) transgenic mice show pancreatic dysfunction resulting in impaired insulin secretion, whereas *Trp53*^{flox/flox} (21) mice and excision repair endonuclease noncatalytic subunit 1 (*Erc1*)^{-/-} (22) mice show adipose tissue senescence and inflammation resulting in insulin resistance, and Sirtuin (*Sirt6*)^{-/-} (23) and *Parp1*^{-/-} (24) mice show increased glucose uptake by skeletal muscle and BAT resulting in increased glucose tolerance. Proposed links between DNA damage with glucose metabolism include modulation of glucose transporters by p53 and through key metabolic regulators such as peroxisome proliferator-activated receptor- γ coactivator (PGC)-1, PARP, and sirtuins (9).

As we have previously shown that replication stress induced by Rev1 deficiency impairs mitochondrial function through NAD⁺ depletion, which could be partially rescued by NR supplementation (12), in this study we aimed to assess whether repletion of NAD⁺ by NR supplementation, a

Figure 5. Schematic overview of proposed mechanisms. Rev1 deletion in mice induces a complex phenotype that is explained by metabolic dysfunction in skeletal muscle as a result of replication stress. This reduces lean mass and locomotor activity, causing a subsequent reduction in energy expenditure, thereby promoting fat mass gain in female mice. Male mice do not develop adiposity, likely due to increased locomotor activity. In female mice, increased dependence on anaerobic glycolysis elevates circulating levels of lactate and as a consequence increases hepatic glucose production, resulting in elevated glucose levels. Excess glucose could further stimulate anaerobic glycolysis in muscle and contribute to increases in fat mass. Male Rev1 KO mice are also hyperglycemic, most likely as a result of increased dependence on anaerobic glycolysis as shown in female mice. KO, knockout. Created with BioRender.com.



precursor of NAD^+ , alleviates metabolic dysfunction. Thereto, Rev1 KO mice and WT littermates were fed either an NR-enriched or standard chow diet. Surprisingly NR supplementation did not improve adiposity or glucose tolerance, despite increased NAD^+ in liver and a tendency toward increased levels in skeletal muscle, indicating that the increased dependency on anaerobic respiration developed early in life persists. In line with previous reports on the use of NR supplementation, no metabolic changes in otherwise healthy WT mice were expected and observed (25–27). Rev1 deletion did likely not reduce NAD^+ content in the tibialis anterior or liver as a whole because NAD^+ depletion by the DNA damage response may primarily occur in proliferating cells. The question remains, however, why NR supplementation did not lead to improvements in the metabolic phenotype in the Rev1 KO mice.

A perspective topic for future studies would be to pinpoint whether the metabolic dysfunction induced by Rev1 deletion results from accumulating damage throughout life, or damage that occurred due to excessive replication stress during intense growth at a young age. Mitochondrial damage that potentially primarily occurs during early life may not be reversed later in life and thereby metabolic impairment could persist. Similar to the early onset of increased adiposity and muscle atrophy observed in Rev1 KO mice, *mdx* mice as a model for Duchenne muscular dystrophy, are characterized by an early onset of muscle dystrophy that does not get progressively worse later in life (28), and by glucose intolerance (29). Similarly, the Rev1 deletion phenotype might develop during growth and stabilize afterward. Future studies should elucidate the metabolic impact of Rev1 deletion in early development versus adulthood, by using inducible or conditional knockout or knock-down models. In addition, it would be of interest to identify the exact mechanism underlying the metabolic phenotype of Rev1 KO mice to determine

whether it may be worthwhile to study the effects of NR supplementation earlier in life.

In conclusion, replication stress caused by Rev1 deletion has pronounced but complex sex-dependent effects on metabolism, most likely initiated by muscular metabolic dysfunction and increased dependence on anaerobic glycolysis.

SUPPLEMENTAL DATA

Supplemental Tables S1–S3 and Supplemental Figs. S1–S5: <https://doi.org/10.6084/m9.figshare.16774813>.

ACKNOWLEDGMENTS

We thank Lemelinda Marques (Department of Human Genetics, Leiden University Medical Center, Leiden, The Netherlands) for excellent technical support.

GRANTS

This work was supported by the Netherlands Cardiovascular Research Initiative: an initiative with support of the Dutch Heart Foundation (CVON-GENIUS-2 to P.C.N.R.). A.T.-S is supported by a grant from the Dutch Cancer Society (KWF 11358).

DISCLOSURES

No conflicts of interest, financial or otherwise, are declared by the authors.

AUTHOR CONTRIBUTIONS

W.I.h.P., A.T.-S., M.S., V.v.H., K.W.v.D., P.C.N.R., N.d.W., and S.K. conceived and designed research; W.I.h.P., M.S., V.v.H., A.C.M.P., T.C.M.S., H.C.M.S., S.A., and S.K. performed experiments; W.I.h.P. analyzed data; W.I.h.P., A.T.-S., M.S. and K.W.v.D., P.C.N.R., N.d.W., and S.K. interpreted results of experiments; W.I.h.P. prepared figures; W.I.h.P. drafted manuscript; A.T.-S., M.S., V.v.H.,

K.W.v.D., P.C.N.R., N.d.W., and S.K., edited and revised manuscript; A.T.-S., M.S., V.v.H., K.W.v.D., P.C.N.R., N.d.W., and S.K., approved final version of manuscript.

REFERENCES

- Yousefzadeh M, Hinpita C, Vyas R, Soto-Palma C, Robbins P, Niedernhofer L. DNA damage-how and why we age? *eLife* 10: e62852, 2021. doi:10.7554/eLife.62852.
- Blackford AN, Jackson SP. ATM, ATR, and DNA-PK: the trinity at the heart of the DNA damage response. *Mol Cell* 66: 801–817, 2017. doi:10.1016/j.molcel.2017.05.015.
- Pilzecker B, Buoninfante OA, Jacobs H. DNA damage tolerance in stem cells, ageing, mutagenesis, disease and cancer therapy. *Nucleic Acids Res* 47: 7163–7181, 2019. doi:10.1093/nar/gkz531.
- Jansen JG, de Wind N. Biological functions of translesion synthesis proteins in vertebrates. *DNA Repair (Amst)* 2: 1075–1085, 2003. doi:10.1016/s1568-7864(03)00119-8.
- Yang IY, Hashimoto K, de Wind N, Blair IA, Moriya M. Two distinct translesion synthesis pathways across a lipid peroxidation-derived DNA adduct in mammalian cells. *J Biol Chem* 284: 191–198, 2009. doi:10.1074/jbc.M806414200.
- Washington MT, Carlson KD, Freudenthal BD, Pryor JM. Variations on a theme: eukaryotic Y-family DNA polymerases. *Biochim Biophys Acta* 1804: 1113–1123, 2010. doi:10.1016/j.bbapap.2009.07.004.
- Martín-Pardillos A, Tsaalbi-Shtylik A, Chen S, Lazare S, van Os RP, Dethmers-Ausema A, Fakouri NB, Bosshard M, Aprigliano R, van Loon B, Salvatori DCF, Hashimoto K, Dingemans-van der Spek C, Moriya M, Rasmussen LJ, de Haan G, Raaijmakers M, de Wind N. Genomic and functional integrity of the hematopoietic system requires tolerance of oxidative DNA lesions. *Blood* 130: 1523–1534, 2017 [Erratum in *Blood* 131: 710, 2018]. doi:10.1182/blood-2017-01-764274.
- Ghosal G, Chen J. DNA damage tolerance: a double-edged sword guarding the genome. *Transl Cancer Res* 2: 107–129, 2013. doi:10.3978/j.issn.2218-676X.2013.04.01.
- Shimizu I, Yoshida Y, Suda M, Minamino T. DNA damage response and metabolic disease. *Cell Metab* 20: 967–977, 2014. doi:10.1016/j.cmet.2014.10.008.
- Rani V, Deep G, Singh RK, Palle K, Yadav UC. Oxidative stress and metabolic disorders: Pathogenesis and therapeutic strategies. *Life Sci* 148: 183–193, 2016. doi:10.1016/j.lfs.2016.02.002.
- Matsuda M, Shimomura I. Increased oxidative stress in obesity: implications for metabolic syndrome, diabetes, hypertension, dyslipidemia, atherosclerosis, and cancer. *Obes Res Clin Pract* 7: e330–e341, 2013. doi:10.1016/j.orcp.2013.05.004.
- Fakouri NB, Durhuus JA, Regnell CE, Angley M, Desler C, Hasan-Olive MM, Martin-Pardillos A, Tsaalbi-Shtylik A, Thomsen K, Lauritzen M, Bohr VA, de Wind N, Bergersen LH, Rasmussen LJ. Rev1 contributes to proper mitochondrial function via the PARP-NAD (+)-SIRT1-PGC1 α axis. *Sci Rep* 7: 12480, 2017 [Erratum in *Sci Rep* 8: 4245, 2018]. doi:10.1038/s41598-017-12662-3.
- De Vos M, Schreiber V, Dantzer F. The diverse roles and clinical relevance of PARPs in DNA damage repair: current state of the art. *Biochem Pharmacol* 84: 137–146, 2012. doi:10.1016/j.bcp.2012.03.018.
- Jansen JG, Langerak P, Tsaalbi-Shtylik A, van den Berk P, Jacobs H, de Wind N. Strand-biased defect in C/G transversions in hypermutating immunoglobulin genes in Rev1-deficient mice. *J Exp Med* 203: 319–323, 2006. doi:10.1084/jem.20052227.
- Parlevliet ET, Heijboer AC, Schröder-van der Elst JP, Havekes LM, Romijn JA, Pijl H, Corssmit EP. Oxyntomodulin ameliorates glucose intolerance in mice fed a high-fat diet. *Am J Physiol Endocrinol Metab* 294: E142–E147, 2008. doi:10.1152/ajpendo.00576.2007.
- Rensen PC, van Dijk MC, Havenaar EC, Bijsterbosch MK, Kruijt JK, van Berkel TJ. Selective liver targeting of antivirals by recombinant chylomicrons—a new therapeutic approach to hepatitis B. *Nat Med* 1: 221–225, 1995. doi:10.1038/nm0395-221.
- Panhuis WIH, Kooijman S, Brouwers B, Verhoeven A, Pronk ACM, Streefland TCM, Giera M, Schrauwen P, Rensen PCN, Schönke M. Mild exercise does not prevent atherosclerosis in APOE*3-Leiden. CETP mice or improve lipoprotein profile of men with obesity. *Obesity (Silver Spring)* 28: S93–S103, 2020. doi:10.1002/oby.22799.
- Chen YW, Harris RA, Hatahet Z, Chou KM. Ablation of XP-V gene causes adipose tissue senescence and metabolic abnormalities. *Proc Natl Acad Sci USA* 112: E4556–E4564, 2015. doi:10.1073/pnas.1506954112.
- Miles PD, Treuner K, Latronica M, Olefsky JM, Barlow C. Impaired insulin secretion in a mouse model of ataxia telangiectasia. *Am J Physiol Endocrinol Metab* 293: E70–E74, 2007. doi:10.1152/ajpendo.00259.2006.
- Hinault C, Kawamori D, Liew CW, Maier B, Hu J, Keller SR, Mirmira RG, Scoble H, Kulkarni RN. $\Delta 40$ Isoform of p53 controls β -cell proliferation and glucose homeostasis in mice. *Diabetes* 60: 1210–1222, 2011. doi:10.2337/db09-1379.
- Shimizu I, Yoshida Y, Moriya J, Nojima A, Uemura A, Kobayashi Y, Minamino T. Semaphorin3E-induced inflammation contributes to insulin resistance in dietary obesity. *Cell Metab* 18: 491–504, 2013. doi:10.1016/j.cmet.2013.09.001.
- Karakasilioti I, Kamileri I, Chatzinikolaou G, Kosteas T, Vergadi E, Robinson AR, Tsamardinos I, Rozgaja TA, Siakouli S, Tsatsanis C, Niedernhofer LJ, Garinis GA. DNA damage triggers a chronic auto-inflammatory response, leading to fat depletion in NER progeria. *Cell Metab* 18: 403–415, 2013. doi:10.1016/j.cmet.2013.08.011.
- Mostoslavsky R, Chua KF, Lombard DB, Pang WW, Fischer MR, Gellon L, Liu P, Mostoslavsky G, Franco S, Murphy MM, Mills KD, Patel P, Hsu JT, Hong AL, Ford E, Cheng HL, Kennedy C, Nunez N, Bronson R, Frendewey D, Auerbach W, Valenzuela D, Karow M, Hottiger MO, Hursting S, Barrett JC, Guarente L, Mulligan R, Dipple B, Yancopoulos GD, Alt FW. Genomic instability and aging-like phenotype in the absence of mammalian SIRT6. *Cell* 124: 315–329, 2006. doi:10.1016/j.cell.2005.11.044.
- Bai P, Cantó C, Oudart H, Brunyánszki A, Cen Y, Thomas C, Yamamoto H, Huber A, Kiss B, Houtkooper RH, Schoonjans K, Schreiber V, Sauve AA, Menissier-de Murcia J, Auwerx J. PARP-1 inhibition increases mitochondrial metabolism through SIRT1 activation. *Cell Metab* 13: 461–468, 2011. doi:10.1016/j.cmet.2011.03.004.
- Shi W, Hegeman MA, van Dartel DAM, Tang J, Suarez M, Swartz H, van der Hee B, Arola L, Keijzer J. Effects of a wide range of dietary nicotinamide riboside (NR) concentrations on metabolic flexibility and white adipose tissue (WAT) of mice fed a mildly obesogenic diet. *Mol Nutr Food Res* 61: 1600878, 2017. doi:10.1002/mnfr.201600878.
- Mitchell SJ, Bernier M, Aon MA, Cortassa S, Kim EY, Fang EF, Palacios HH, Ali A, Navas-Enamorado I, Di Francesco A, Kaiser TA, Waltz TB, Zhang N, Ellis JL, Elliott PJ, Frederick DW, Bohr VA, Schmidt MS, Brenner C, Sinclair DA, Sauve AA, Baur JA, de Cabo R. Nicotinamide improves aspects of healthspan, but not lifespan, in mice. *Cell Metab* 27: 667–676.e4, 2018. doi:10.1016/j.cmet.2018.02.001.
- Crisol BM, Veiga CB, Lenhare L, Braga RR, Silva VRR, da Silva ASR, Cintra DE, Moura LP, Pauli JR, Ropelle ER. Nicotinamide riboside induces a thermogenic response in lean mice. *Life Sci* 211: 1–7, 2018. doi:10.1016/j.lfs.2018.09.015.
- Grounds MD. Two-tiered hypotheses for Duchenne muscular dystrophy. *Cell Mol Life Sci* 65: 1621–1625, 2008. doi:10.1007/s00018-008-7574-8.
- Stapleton DI, Lau X, Flores M, Trieu J, Gehrig SM, Chee A, Naim T, Lynch GS, Koopman R. Dysfunctional muscle and liver glycogen metabolism in mdx dystrophic mice. *PLoS One* 9: e91514, 2014. doi:10.1371/journal.pone.0091514.